Raman spectroscopy of neutron irradiated silicon carbide: correlation among Raman spectra, swelling and irradiation temperature*

T. Koyanagi, Y. Katoh, M.J. Lance

Materials Science and Technology Division, Oak Ridge National Laboratory, Oak Ridge, TN 37831, USA

Abstract

The effects of neutron irradiation on microstructural evolution and the resultant changes in physical and mechanical properties are of critical importance for the development of silicon carbide (SiC) materials for nuclear applications. This study neutron-irradiated β-SiC under a wide range of conditions at temperatures between 235 and 750°C and neutron doses of 0.01–11.8 displacements per atom, and then evaluated the effects on the SiC structure using Raman spectroscopy. The SiC optical phonon lines were shifted to lower wavenumbers by irradiation. Correlations were found among the wavenumber of the longitudinal optical phonon line, irradiation-induced swelling, and irradiation temperature. The peak shift also correlated indirectly with decreasing thermal conductivity of irradiated SiC. The irradiation-induced peak shift is explained by combinations of lattice strain, reduction of the elastic modulus, and other factors including decreasing coherent domain size. These findings bridge irradiation-induced microstructural changes and property changes and illustrate how Raman spectroscopy is a useful tool for nondestructively assessing irradiated SiC materials for nuclear applications.

Keywords

Silicon carbide, Neutron irradiation, Irradiation defects, Swelling, Nuclear

---

Introduction

Silicon carbide (SiC) based materials have been explored for various nuclear structural and functional applications including core and fuel components of advanced fission reactors, fuel cladding of light water reactors, and fusion reactor components [1–3]. This is because SiC present various inherent advantages over candidate or currently used metallic materials, including high-temperature strength, chemical stability, and low neutron absorption [4]. In nuclear reactor environments, high-energy neutrons are produced in nuclear fission or fusion reactions. The effects of neutron irradiation on SiC are of great interest in nuclear applications [1,2] because the energetic neutrons introduce atomic displacements in the material and the resultant atomistic defects greatly affect in-pile performance through changes in dimensional stability, mechanical properties, and thermal conductivity [2]. In addition, understanding and controlling irradiation-induced defects is key to semiconductor and optical applications in which SiC is subjected to ion irradiation during processing to tailor its physical properties [5]. Therefore, the evolution of irradiation defects in SiC is of great interest.

Raman spectroscopy has been widely employed to assess the microstructure and properties of SiC in various forms. For example, it has been used to evaluate polytypes [6], crystalline size [7], stoichiometry and processing impurities [8], elastic strain [9,10], mechanical properties [11], temperature[12], amorphous-like nanostructure[13,14], and stacking fault defects [15]. Raman spectroscopy is also useful for analyzing irradiation induced microstructural changes in SiC, including amorphization [16], chemical disordering [16], irradiation-induced lattice strain [17], and changes in electrical properties [18].

We measured the Raman spectra of SiC following neutron irradiation under various temperature and dose conditions. The objective is development of nondestructive techniques to probe and quantify the structural disorder in SiC to assess its material performance in nuclear reactor environments. More specifically, we investigated the correlation between the Raman peak positions and irradiation-induced swelling. Swelling is not only a key property, which is highly dependent on irradiation temperature and a cause of significant stress within the component if temperature gradients exist [19,20], but also is known to be correlated with irradiation-induced modification of other properties, including elastic constants and thermal conductivity. Swelling of SiC is known to be a resultant of lattice expansion in case of the irradiation conditions studied as explained later. Therefore, we discuss relationship between Raman peak shift and lattice expansion and do not focus on the other factors affecting swelling including irradiation-induced

amorphization, dislocation loop growth, and void formation. In addition, we evaluated the irradiation-temperature dependence of peak shifts in the Raman spectra. Therefore, this paper provides a comparison of Raman spectra, swelling, and irradiation temperatures of SiC for various irradiation conditions up to relatively high neutron doses, which have not heretofore been sufficiently studied. Such information will be useful for probing irradiated SiC materials by Raman spectroscopy.

Experimental methods

Polycrystalline, chemical vapor deposited (CVD) β-SiC (high resistivity grade, Dow Chemical Co., Marlborough, Massachusetts) was used as the test material. The material purity was 99.9995%, guaranteed by the manufacturer. The processing defects, other than the impurity elements, include grain boundaries, twin boundaries, and stacking faults [21]. The average coherent domain size of ~200 nm was confirmed by X-ray diffraction (XRD) [22], and nearly isotropic grain growth was observed [21]. The CVD SiC material was machined to a thin plate with dimensions of 50 × 5 × 0.2 mm. The specimens were neutron-irradiated in the High Flux Isotope Reactor at Oak Ridge National Laboratory to total fluences of 0.01–11.8 × 10^{25} n/m^2 (E > 0.1 MeV) in an inert gas atmosphere (helium or neon). An equivalence of one displacement per atom (dpa) = 1 × 10^{25} n/m^2 (E > 0.1 MeV) is assumed in this study [23]. The neutron flux was ~1 × 10^{19} n/m^2/s. The irradiation temperatures ranged between 235 and 750°C, as determined by post-irradiation annealing of the specimen using dilatometry [24]. These temperatures are above the radiation-induced amorphization temperature of SiC (~150°C) [2]. The accuracy of the temperature determination was 10–15°C [24].

The specimens were excited by the 532 nm line of an argon ion laser focused to a spot 2–3 μm in size on the specimen, using a 50× microscope objective lens. This spot size correlates to ~100 coherent domains. The laser power used was 2.5 mW. Raman spectra were collected in a backscattering geometry and dispersed using a Renishaw inVia confocal Raman microscope. Five to ten spectra were collected from each specimen, with all measurements conducted at room temperature. The dimensional change of the specimens due to irradiation was evaluated using a micrometer with a precision of <1 μm, which measured length swelling to an accuracy of <0.01%.

Results

Fig. *1* shows changes in the Raman spectra of β-SiC following neutron irradiation at ~500°C. The top Raman spectrum of Fig. 1 is from an unirradiated specimen of SiC and is shown for comparison. The Raman spectrum of the pristine SiC shows

transverse optical (TO) and longitudinal optical (LO) phonon lines of β-SiC at around 795 and 970 cm^{-1}, respectively. In the irradiated spectra, additional broad bands at ~520, ~1400, and ~1600 cm^{-1} were found, which were absent in the reference spectrum. Those peaks are reportedly attributed to vibrations of Si-Si (~520 cm^{-1}) and C-C (~1400 and ~1600 cm^{-1}) bonds [16], and are an indication of the local decomposition of SiC crystal. Analysis of these homonuclear bond peaks is beyond the scope of this work.

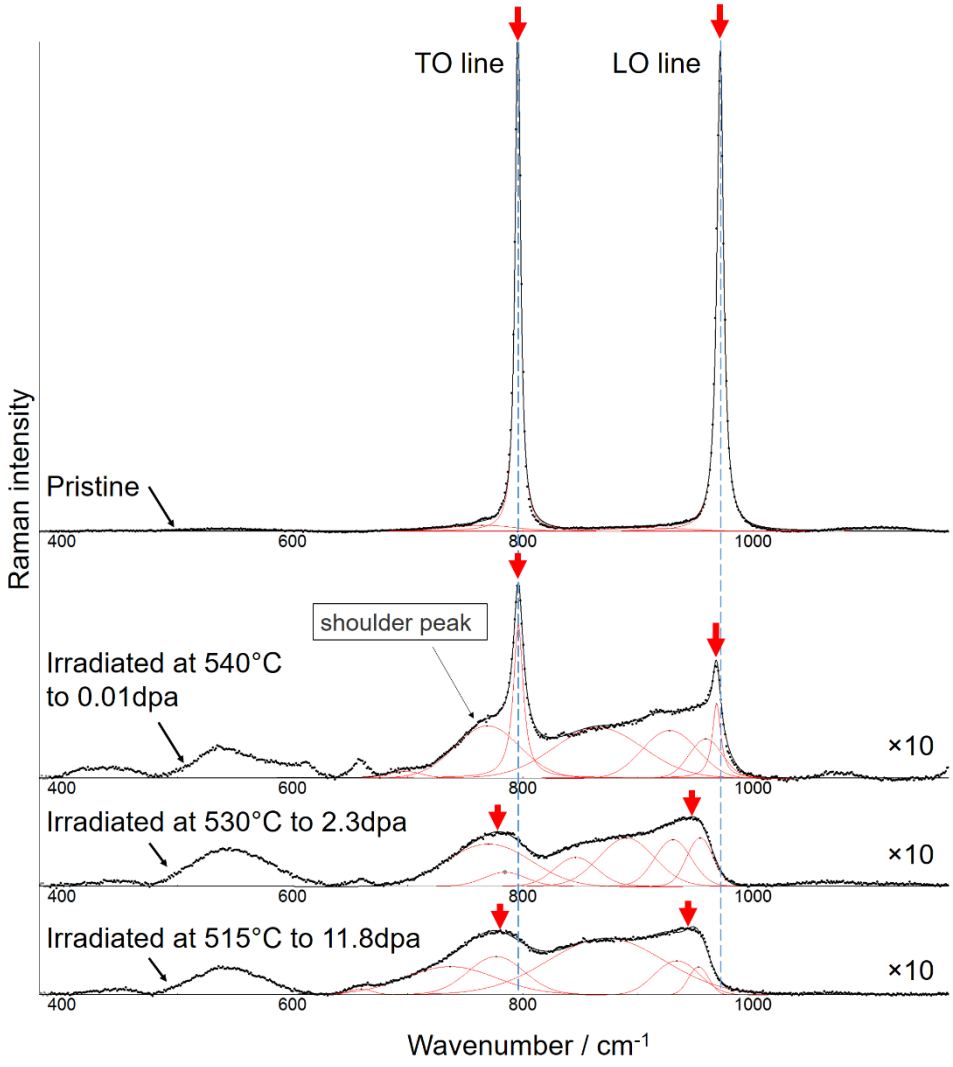

Fig. 1 Raman spectra of β-SiC neutron irradiated at ~500°C to 0.01–11.8dpa. The intensities of the irradiated SiC spectra are magnified ten-fold. Red arrows indicate peak positions of raw spectra used for peak-shift analysis in Fig.2 and 4.

With increasing neutron dose, both the TO and the LO peaks were weakened, broadened, and shifted to a lower wavenumber. These irradiation-produced changes were

also observed in previous work on neutron and ion irradiated SiC [16,25]. It was clearly seen that a shoulder peak at 770–780 cm^{-1}, very small in the unirradiated material, was associated with a sharp TO line following irradiation at 0.01 dpa, and the shoulder peak appeared to be dominant beyond 2.3 dpa. In all cases, the sharp TO and LO bands were well fitted with a Lorentzian function. The other bands between 600 and 1000 cm^{-1} were fitted with a mixed Lorentzian-Gaussian function, and a total of six or seven bands were required. Since conventional fitting does not provide absolute TO and LO peak positions, especially in high-dose cases, the peak position of the raw spectrum was used to evaluate peak shifting due to neutron irradiation in this study. Fig. 2 shows the peak position of the TO peak at 775–800 cm^{-1} plotted against the linear swelling due to dimensional change in the specimen. The results from previous work are also plotted [17]. The wavenumber of the peak position decreases linearly with increasing swelling up to ~0.4 %. Above this value, the peak position is insensitive to swelling and remained at ~780 cm^{-1}. The LO peak position is also plotted against swelling. The behavior is different from that of the TO line; the peak position monotonically decreases with increasing swelling up to ~0.7%.

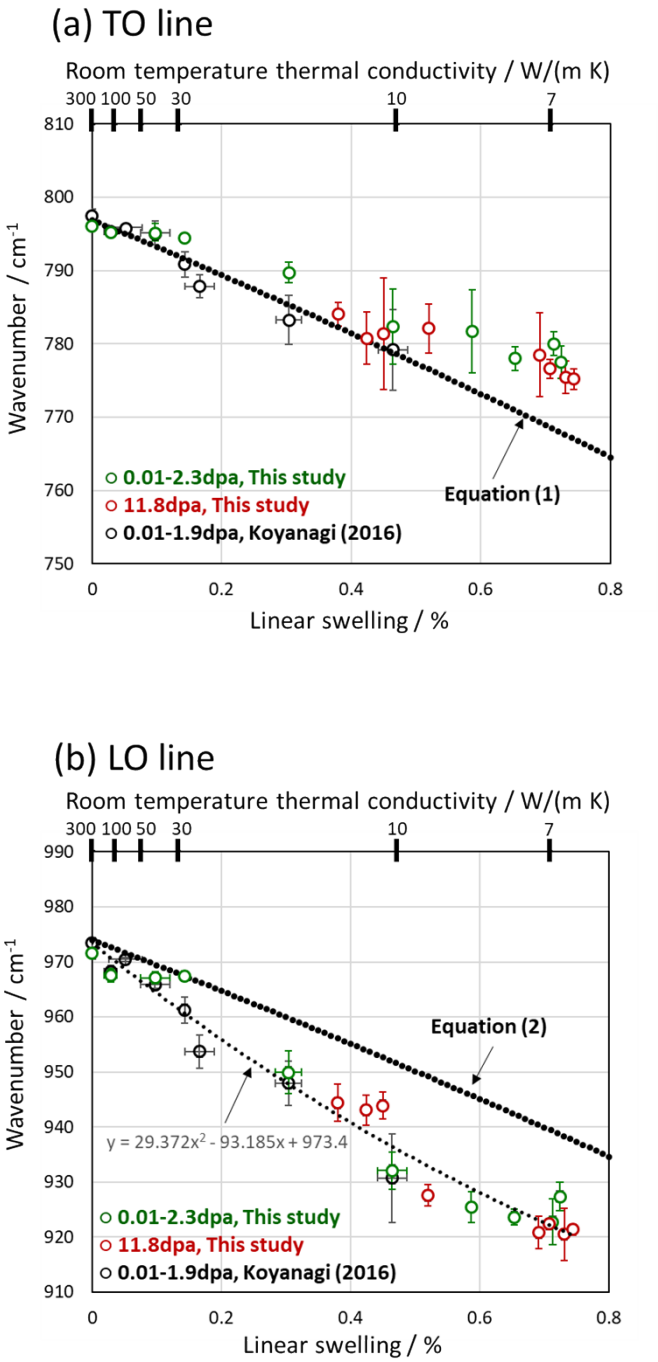

Fig. 2 Swelling dependence of TO (a) and LO (b) Raman phonon lines of neutron irradiated β-SiC. Swelling was evaluated via the dimensional change in the specimen. The graph also shows that correlation between the Raman phonon lines and the room-temperature thermal conductivity, which was estimated from the swelling [2]. Equations (1) and (2) are discussed later in the paper.

Irradiation temperature also affected the Raman peak position. Fig. 3 compares

the Raman spectra of SiC nonirradiated and irradiated at 250 and 600°C to ~2 dpa. The broad LO peak clearly shifted to a lower wavenumber by decreasing irradiation temperature. On the other hand, the peak position of the broad TO band was less sensitive to irradiation temperature. Fig. *4* shows the dependence of the LO peak position on irradiation temperature. The neutron dose varied from 2.0 to 11.8 dpa. The peak position was shifted to a lower wavenumber as irradiation temperature decreased below 750°C, regardless of the neutron dose. All the data, including reported data for irradiated CVD β-SiC [17], were well fitted by a linear trendline. Fig. *4* also shows temperature-dependent swelling. The swelling linearly decreased with increasing irradiation temperature, as reported in previous work, as a result of the increased probability of defect annihilations at higher temperatures [2]. There was no clear relationship between the peak position of the TO line and the irradiation temperature at doses of 2.0–11.8 dpa.

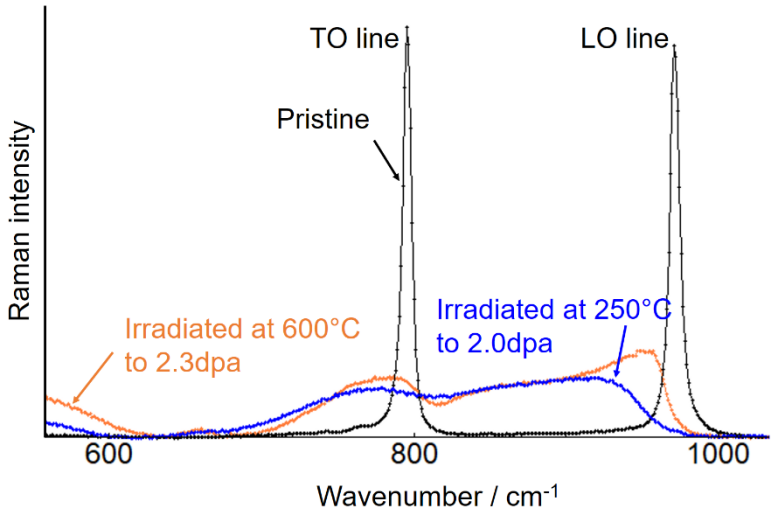

Fig. 3 Irradiation temperature dependence of Raman spectra of β-SiC neutron irradiated to ~2 dpa.

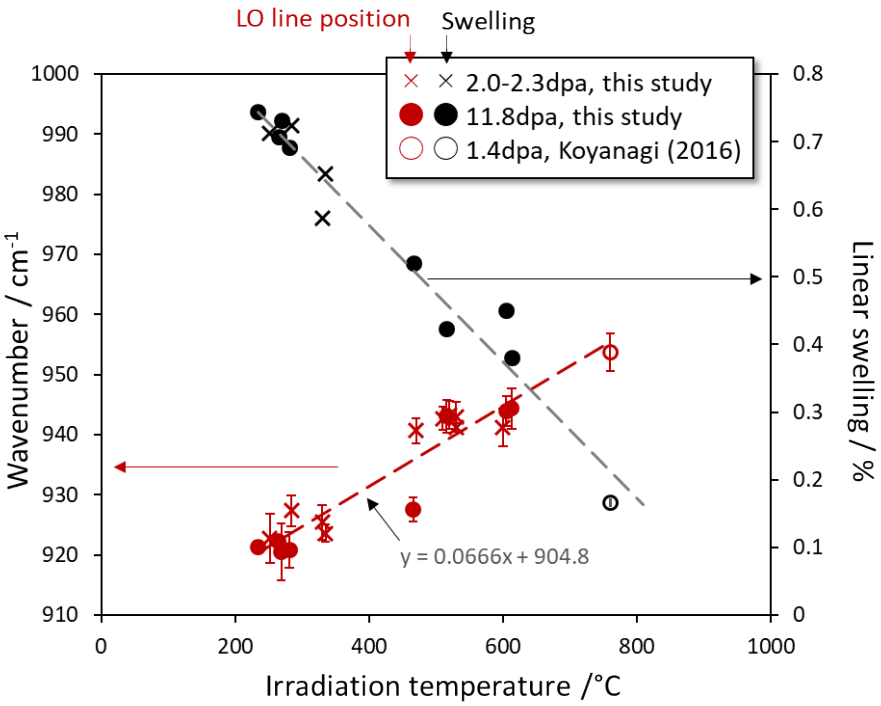

Fig. 4 Irradiation temperature dependence of LO peak position and swelling of β-SiC neutron irradiated to 1.4–11.8 dpa. Note that, in this study, the same specimen was used for Raman characterization and dilatometry to determine the irradiation temperature.

Discussion

We found a correlation between the TO and LO peak positions and irradiation-induced swelling across a wide range of temperatures and dose conditions (Fig. 2). It is also possible that Raman spectroscopy probes the thermal conductivity of irradiated SiC, as shown in Fig. 2a and b, because of the known empirical correlation between swelling and the room-temperature thermal conductivity of irradiated SiC [2]. The empirical relationship between swelling and thermal conductivity of neutron-irradiated SiC is supported by a larger set of data shown in reference [2]. In short, the thermal conductivity monotonically decreases with increasing the swelling. The result of this study is consistent with previous study on Raman spectroscopy of irradiated SiC, showing the TO and LO peak positions of 795 and 971 cm^{-1}, respectively, for the thermal conductivity of 150–250 W/(m K) [26]. Therefore, the Raman peak positions are indirectly correlated with room–temperature thermal conductivity, though a theoretical explanation is currently lacking. Several factors associated with phonon scattering could be considered for a theoretical explanation [27], which is a research area for future study. In addition, Fig. *4* indicates that Raman spectroscopy enables post-irradiation evaluation of the irradiation

temperature of SiC. Since swelling, thermal conductivity, and irradiation temperature are all key properties or parameters for assessing material performance in irradiation environments [2], this finding highlights the usefulness of Raman spectroscopy as a nondestructive evaluation tool for assessing of irradiated SiC. The following sections describe how to interpret the changes in the Raman peak positions due to irradiation.

This study found significant changes in the Raman spectra of SiC from the pristine vs. the neutron-irradiated conditions. Such changes are associated with the formation of irradiation-induced defects that do not completely destroy the crystalline feature but decrease the coherent grain size as the neutron dose increases, neutron dose based on XRD [22]. The TO and LO peak shifts observed in this study can be affected by several factors, including elastic strain, which generally causes a peak shift to a lower wavenumber under tension. In SiC, the presence of irradiation–induced atomistic defects such as interstitial, vacancy, and anti-site type defects results in elastic strain [28]. Olego et al. studied the effect of elastic strain on phonon Raman bands of β-SiC and found a linear correlation between the Raman peak positions and elastic strain [9]. To apply Olego's finding to the Raman spectra of irradiated SiC, Koyanagi et al. modified this Raman peak position–elastic strain relationship by considering the reduction in the elastic constant of SiC due to irradiation defects [17], because radiation defects decrease the elastic modulus of SiC. This reduction in the elastic modulus is explained by weakening of the atomic bonding due to lattice expansion [2]. The wavenumber (ω) of the TO and LO modes under elastic strain can be expressed (in units of cm^{-1}) by

$$\omega(TO) = 797 - 3734\frac{E_{unir}}{E_{irr}}\frac{(a_{irr} - a_{unir})}{a_{unir}}, \quad (1)$$

$$\omega(LO) = 973 - 4532\frac{E_{unir}}{E_{irr}}\frac{(a_{irr} - a_{unir})}{a_{unir}}, \quad (2)$$

where a and E are lattice constant and Young's modulus, respectively, at room temperature. The subscripts *unir* and *irr* indicate properties of unirradiated and irradiated materials, respectively. The lattice constant of irradiated SiC was obtained from macroscopic swelling assuming the lattice expansion is fully responsible to macroscopic swelling. This assumption is acceptable for irradiation condition for the dose of up to ~10 dpa, according to previous x-ray diffraction work on neutron-irradiated SiC [29]. In cases of irradiation to such dose levels, dominant small defect clusters and point-defects contribute to both lattice and macroscopic swelling, according to refs [2,29]. In irradiated SiC, irradiation defects will increase the strain-induced peak shift, which is related to the

anharmonicity of the atomic bonding, i.e. the decrease in the Young's modulus. The change in modulus due to radiation between ~150–~1000°C is given by [2]

$$E_{irr} = E_{unir}(1 - 6.974S), \quad (3)$$

where S is irradiation temperature and dose dependent volumetric swelling was mostly the result of lattice expansion[29]. The reduction in the Young's modulus was up to 15.6% in this study. Given that the modulus change depends on swelling, Eq. (1) presents swelling dependent SiC optical phonon lines.

Equation (1) explains the swelling-dependent TO peak position up to the linear swelling level of ~0.4% in Fig. 2a. This strongly indicates that the combined effect of elastic strain attributed to swelling and the reduction of the modulus caused the peak shift. Above this swelling level, the peak position was less sensitive to the swelling and remained within the range of 775–785 cm^{-1}. Since lattice expansion equal to the macroscopic swelling of irradiated SiC was confirmed at up to 2.6% using X-ray diffraction [30], it was unexpected that Eq. (1) would not fully explain the peak shift at higher swelling levels. It may have failed to do so because the TO peak shift was apparently lower than the value derived from Eq. (1), which was due to peak overlapping between the TO line and the shoulder peak shown in Fig. 1. The shoulder peak is reported to be due to the high-density stacking fault disorder and/or the phonon confinement effect due to the decreasing coherent domain size (< ~1 nm) of β-SiC [15,31]. This assumption is supported by the similar peak positions among the apparent TO line and the shoulder lines at swelling levels beyond ~0.4%. Therefore, Eq. (1) is useful for probing irradiated SiC with swelling of less than ~0.4 %.

In the case of the LO line, the peak was shifted beyond the expectation based on Eq. (2). Our previous study [17] concluded that this additional peak shift can be interpreted as a phonon confinement effect resulting in a decreasing correlation length with increasing defect density. In ideal single crystals, only the Brillouin-zone-center optical phonons can be observed using Raman spectroscopy. However, this selection rule is relaxed owing to the interruption of lattice periodicity in a material with a nano-scale coherent domain size, causing the Raman spectrum also to have contributions from phonons away from the zone center [32]. The result was the shift of the SiC LO line to a lower wavenumber [17]. The smaller the coherent grain size due to defects, the greater the shift of the LO line owing to the phonon confinement effect. Because the gap between the peak shifts of the experiment and the results of Eq. (2) grew larger with increasing

swelling in Fig. 2, the larger swelling was associated with a microstructure with smaller coherent grain size. This was consistent with a previous study using electron microscopy that found that a higher density of the defects in SiC exhibited larger swelling [33]. Moreover, it was found that an additional emergent peak around 940 cm^{-1} due to irradiation caused the LO peak to shift lower [17].

It is also possible that the LO peak position was affected by free carriers [34]. One of the free carrier sources was transmutation element, which was the donor of the SiC semiconductor. However, the major solid transmutation element of phosphorus was produced by only 6 appm/dpa (5×10^{16} cm^{-3}/dpa) based on simulation [35]. The effect on the Raman peak shift of donor production at such low density was much less significant than the shift found in this study [34]. Radiation defects with charged states in SiC may also affect the Raman spectra. The knowledge regarding this effect is currently limited [36].

Irradiation temperature is known to greatly affect the swelling of SiC; the higher the temperature, the lower the swelling as shown in Fig. 4. This effect is a result of the increased probability of vacancy-interstitial recombination at high temperature via increased defect mobility. Since the LO peak position/swelling and swelling/irradiation temperature both are correlated, it is reasonable to assume that the peak position and irradiation temperature was also correlated at the same dose level. The larger peak shift at lower irradiation temperature is explained by a combination of larger elastic strain and smaller correlation length. It is possible to determine the irradiation temperature of SiC with an unknown radiation history from the LO phonon line based on the linear fit of the data in Fig. 4 , to an accuracy of ± 55°C within a 95% confidence interval.

Our interpretation is that the LO and TO Raman peak shifts due to irradiation can be attributed to a combination of elastic strain equivalent to swelling, a reduction in the elastic modulus, and decreased correlation length. The correlation we found is expected to be valid as long as swelling is caused by lattice expansion (elastic strain), i.e., below temperatures that result in void swelling with limited lattice expansion (~1000°C) [2]. Although further Raman study may be needed for complete correlation between the Raman lines and the properties of SiC irradiated at very high temperatures, the present study demonstrated the usefulness of Raman spectroscopy for probing SiC irradiated between 235 and 750°C.

This study also investigated the correlation between Raman spectra and the effects of irradiation on SiC based on Raman intensity, although that correlation was not clear. The intensity of first-order lines of irradiated SiC normalized to those of pristine SiC has been proposed to be the degree of disordering [16], which was relevant to the

number of displaced atoms deduced from Rutherford backscattering spectrometry [37]. Importantly, this level of disordering was a key to characterizing the dimensional stability of ion-irradiated SiC at room temperature and at 400°C, as reported by Kerbiriou et al. [38]. In this study, the Raman intensity of irradiated SiC relative to nonirradiated SiC was not sufficiently sensitive to correlate the Raman spectra and the properties of SiC under the irradiation conditions investigated. There may be opportunities to correlate the relative Raman intensity and the effects of irradiation on SiC under different irradiation conditions (e.g. lower temperatures and doses) because of the proven correlation between the amount of disordering and the dimensional stability [38].

Conclusions

We found empirical correlations among Raman phonon line positions, swelling, and irradiation temperature for high-purity β-SiC ceramics exposed to reactor neutron irradiation to 0.01–11.8 dpa at 235–750°C. In addition, the thermal conductivity of the irradiated SiC was indirectly correlated to the phonon peak positions, based on the known correlation between swelling and thermal conductivity. These findings are useful for nondestructively probing and assessing neutron irradiation effects on SiC for nuclear applications.

The changes in the TO line position due to neutron bombardment were interpreted based on the combined effects of lattice strain and change in elastic modulus. In the case of a higher swelling level and the LO line, additional factors affected the peak shifting, including the phonon confinement effect caused by decreasing coherent domain size due to radiation-produced defects in the SiC. This microstructural information regarding SiC neutron-irradiated under various conditions is a useful addition to the knowledge base on radiation defect evolution in SiC.

Acknowledgements

This work was sponsored by the U.S. Department of Energy (DOE), Office of Nuclear Energy, Nuclear Science User Facilities program and the Advanced Fuel Campaign of the Nuclear Technology Research & Development program under contact DE-AC05-00OR22725 with Oak Ridge National Laboratory (ORNL) managed by UT Battelle, LLC. Part of the irradiation was supported by the Office of Fusion Energy Sciences, DOE. A portion of this research used resources at the High Flux Isotope Reactor, a DOE Office of Science User Facility operated by the ORNL. Jagjit Nanda and Frederick Wiffen (ORNL) provided useful comments on the manuscript.

References

[1] Y. Katoh, L. L. Snead, C. H. Henager, T. Nozawa, T. Hinoki, A. Iveković, S. Novak, S. M. Gonzalez De Vicente, *J. Nucl. Mater.* **2014**, *455*, 387.

[2] L. L. Snead, T. Nozawa, Y. Katoh, T. S. Byun, S. Kondo, D. A. Petti, *J. Nucl. Mater.* **2007**, *371*, 329.

[3] K. A. Terrani, J. O. Kiggans, Y. Katoh, K. Shimoda, F. C. Montgomery, B. L. Armstrong, C. M. Parish, T. Hinoki, J. D. Hunn, L. L. Snead, *J. Nucl. Mater.* **2012**, *426*, 268.

[4] C. Sauder, in *Ceramic Matrix Composites: Materials, Modeling and Technology*, **2014**, pp. 609–646.

[5] J. B. Casady, R. W. Johnson, *Solid. State. Electron.*, **1996**, 39, 1409–1422.

[6] S. Nakashima, H. Harima, *Phys. Status Solidi Appl. Res.* **1997**, *162*, 39.

[7] Y. Sasaki, Y. Nishina, M. Sato, K. Okamura, *Phys. Rev. B* **1989**, *40*, 1762.

[8] Y. Sasaki, Y. Nishina, M. Sato, K. Okamura, *J. Mater. Sci.* **1987**, *22*, 443.

[9] D. Olego, M. Cardona, *Phys. Rev. B* **1982**, *25*, 1151.

[10] G. Gouadec, P. Colomban, N. P. Bansal, *J. Am. Ceram. Soc.* **2001**, *84*, 1136.

[11] G. Gouadec, P. Colomban, *J. Eur. Ceram. Soc.* **2001**, *21*, 1249.

[12] D. Olego, M. Cardona, *Phys. Rev. B* **1982**, *25*, 3889.

[13] M. Havel, P. Colomban, *J. Raman Spectrosc.* **2003**, *34*, 786.

[14] M. Havel, D. Baron, P. Colomban, *J. Mater. Sci.* **2004**, *39*, 6183.

[15] S. Rohmfeld, M. Hundhausen, L. Ley, *Phys. Rev. B* **1998**, *58*, 9858.

[16] S. Sorieul, J. M. Costantini, L. Gosmain, L. Thomé, J. J. Grob, *J. Phys. Condens. Matter* **2006**, *18*, 5235.

[17] T. Koyanagi, M. J. Lance, Y. Katoh, *Scr. Mater.* **2016**, *125*, 58.

[18] T. Mitani, S. I. Nakashima, K. Kojima, T. Kato, H. Okumura, *J. Appl. Phys.* , DOI:10.1063/1.4748279.

[19] M. Ben-Belgacem, V. Richet, K. A. Terrani, Y. Katoh, L. L. Snead, *J. Nucl. Mater.* **2014**, *447*, 125.

[20] J. G. Stone, R. Schleicher, C. P. Deck, G. M. Jacobsen, H. E. Khalifa, C. A. Back, *J. Nucl. Mater.* **2015**, *466*, 1.

[21] Y. Katoh, L. L. Snead, C. M. Parish, T. Hinoki, *J. Nucl. Mater.* **2013**, *434*, 141.

[22] D. J. Sprouster, T. Koyanagi, E. Dooryhee, S. K. Ghose, Y. Katoh, L. E. Ecker, *Scr. Mater.* **2017**, *137*, 132.

[23] G. Newsome, L. L. Snead, T. Hinoki, Y. Katoh, D. Peters, *J. Nucl. Mater.* **2007**, *371*, 76.

[24] A. A. Campbell, W. D. Porter, Y. Katoh, L. L. Snead, *Nucl. Instruments Methods Phys. Res. Sect. B Beam Interact. with Mater. Atoms* **2016**, *370*, 49.
[25] P. F. Wang, L. Huang, W. Zhu, Y. F. Ruan, *Solid State Commun.* **2012**, *152*, 887.
[26] V. S. Chauhan, M. F. Riyad, X. Du, C. Wei, B. Tyburska-Püschel, J.-C. Zhao, M. Khafizov, *Metall. Mater. Trans. E* **2017**, *4*, 61.
[27] M. G. Holland, *Phys. Rev.* , DOI:10.1103/PhysRev.134.A471.
[28] A. Debelle, A. Boulle, A. Chartier, F. Gao, W. J. Weber, *Phys. Rev. B - Condens. Matter Mater. Phys.* , DOI:10.1103/PhysRevB.90.174112.
[29] T. Yano, H. Miyazaki, M. Akiyoshi, T. Iseki, *J. Nucl. Mater.* **1998**, *253*, 78.
[30] L. L. Snead, Y. Katoh, T. Koyanagi, K. Terrani, E. D. Specht, *J. Nucl. Mater.* , DOI:10.1016/j.jnucmat.2016.01.010.
[31] S. Rohmfeld, M. Hundhausen, L. Ley, *Phys. Status Solidi Basic Res.* **1999**, *215*, 115.
[32] A. K. Arora, M. Rajalakshmi, T. R. Ravindran, V. Sivasubramanian, *J. Raman Spectrosc.*, **2007**, 38, 604–617.
[33] Y. Katoh, N. Hashimoto, S. Kondo, L. L. Snead, A. Kohyama, *J. Nucl. Mater.* **2006**, *351*, 228.
[34] H. Yugami, S. Nakashima, A. Mitsuishi, A. Uemoto, M. Shigeta, K. Furukawa, A. Suzuki, S. Nakajima, *J. Appl. Phys.* **1987**, *61*, 354.
[35] H. L. Heinisch, L. R. Greenwood, W. J. Weber, R. E. Williford, *J. Nucl. Mater.* **2004**, *327*, 175.
[36] G. Roma, *Phys. status solidi* **2016**, *213*, 2995.
[37] R. Menzel, K. Gärtner, W. Wesch, H. Hobert, *J. Appl. Phys.* **2000**, *88*, 5658.
[38] X. Kerbiriou, J. M. Costantini, M. Sauzay, S. Sorieul, L. Thoḿ, J. Jagielski, J. J. Grob, *J. Appl. Phys.* , DOI:10.1063/1.3103771.